Supporting Information

On-Chip Monitoring of toxic gases: capture and label-free SERS detection with plasmonic mesoporous sorbents

Marta Lafuente,[†,§] Fernando Almazán,[†,§] Eduardo Bernad,[†,§] Ileana Florea,[#] Raul Arenal,[†,‡,+] Miguel A. Urbiztondo,[⊥] Reyes Mallada,[†,§,‖] M. Pilar Pina,[,†,§,‖]*

[†]Instituto de Nanociencia y Materiales de Aragón (INMA), CSIC-Universidad de Zaragoza, 50009 Zaragoza, Spain.

[§]Department of Chemical & Environmental Engineering, Edificio I+D+i, Campus Rio Ebro, C/Mariano Esquillor s/n, 50018 Zaragoza, Spain

#Laboratoire de Physique des Interfaces et des Couches Minces (LPICM), CNRS, Ecole Polytechnique, IP Paris, 91128, Palaiseau Cedex, France

[‡] ARAID Foundation, 50018 Zaragoza, Spain

[+]Laboratorio de Microscopias Avanzadas (LMA), Universidad de Zaragoza, 50018 Zaragoza, Spain.

[⊥] Centro Universitario de la Defensa de Zaragoza, Carretera Huesca s/n, 50090 Zaragoza, Spain.

[‖] Networking Research Center on Bioengineering, Biomaterials and Nanomedicine, CIBER-BBN, 28029 Madrid, Spain.

Section 1. Fabrication and Characterization of the SERS microfluidic chip

Microfabrication Process

The microfabrication process for the functional microfluidic SERS chip comprises five different steps: cavity etching, plasmonic sorbent material incorporation, microdevice sealing, heater element integration and inlet/outlet ports mechanization (Figure S1.1):

1) **Microchannel definition on Si substrate.** As previously described[1], the anisotropic wet etching of a microchannel on P doped Si wafers (500 ± 20 μm thickness, <100> crystal orientation, 5 - 10 Ω·cm resistivity) supplied by Sil'Tronix is carried out. Open microchannels of 5 mm x 33 mm and 40 μm in depth are defined by anisotropic Si etching in KOH 40 %w/v at 80 ºC for 40 min using a specific negative-working photoresist ProTEK (Brewer Science). The total free volume of the cavity is 5.9 μL. The optical masks were designed using Clewin5® software and printed on high grade acetate film by Micro Lithography Services LTD.

2) **Deposition of plasmonic mesoporous sorbent in the microchannel.** The core-shell "MCM48-Au seeds" and "MCM48@Au" nanoparticles are incorporated inside the microfluidic cavity by 25 cycles of spin coating with the corresponding ethanolic solutions 0.15 % wt. To avoid spillage of material all over the top-surface, the microfluidic chip is protected with a custom, pre-cut adhesive tape which upon exposure to UV is easily peeled off. Each spin coating cycle comprises the following steps: *(i)* dispersion of the solution (25 μL) over the substrate at low angular speed (Ω = 300 rpm) for 15 s; and *(ii)* evaporation of the solvent at high angular speed (Ω = 1000 rpm) for 60 s. Finally, thermal annealing is carried out at 80 ºC for 2 min.
3) **Sealing of the functionalized microchannel with Borofloat glass substrate by anoding bonding**. The Si and glass parts of the microfluidic chip are assembled and

sealed by anodic bonding overnight at 1000 V - 250 ºC. The Borofloat wafer (500 µm thick) supplied by Siegert Wafer GmbH was cleaned before use by immersing consecutively for 2 min on an ultrasonic bath with acetone, ethanol, and water and dried with N_2.

4) **Heating coil definition on the microfluidic device.** The last step in the microfluidic SERS chip fabrication is the incorporation of a heating type resistor and a temperature sensing probe on the Si back side. This was carried out by a standard lift-off process with 150 nm of Au layer (with an adhesion layer of 50 nm Cr) deposited by Electron Bean Physical Vapor Deposition (EBPVD) (Edwards auto-500) and a standard photolithography resist (TI35ESX, MicroMechanics) used as a sacrificial layer. To guarantee electric isolation all over the back side of the Si wafer, a 100 nm layer of Al_2O_3 in direct contact with the Si wafer was firstly deposited by EBPVD. Thus, the in-situ degassing of the plasmonic sorbent is performed by applying adequate DC voltage to the printed heater. Each 4-inch Si wafer contains 8 different microdevices substrates, which are diced apart after the process is finished. The dimensions of each microdevice are 15 mm × 43 mm (width × length).

5) **Microfluidic Connections.** Inlet/outlet ports are mechanized on top of the glass cover by sandblasting. Transfer lines of fused silica capillaries (320 µm-diameter) are inserted through high temperature septa (Thermogreen LB-2 Septa) glued to the glass substrate with thermoresistant silicone (Acc Silcoset 158, Tmax = 300 ºC). The dimensions of the optical window, delimited by inlet/outlet fluidic ports, are compatible with the benchtop and portable Raman instrumentation used in this work for the SERS measurements in flow.

a)

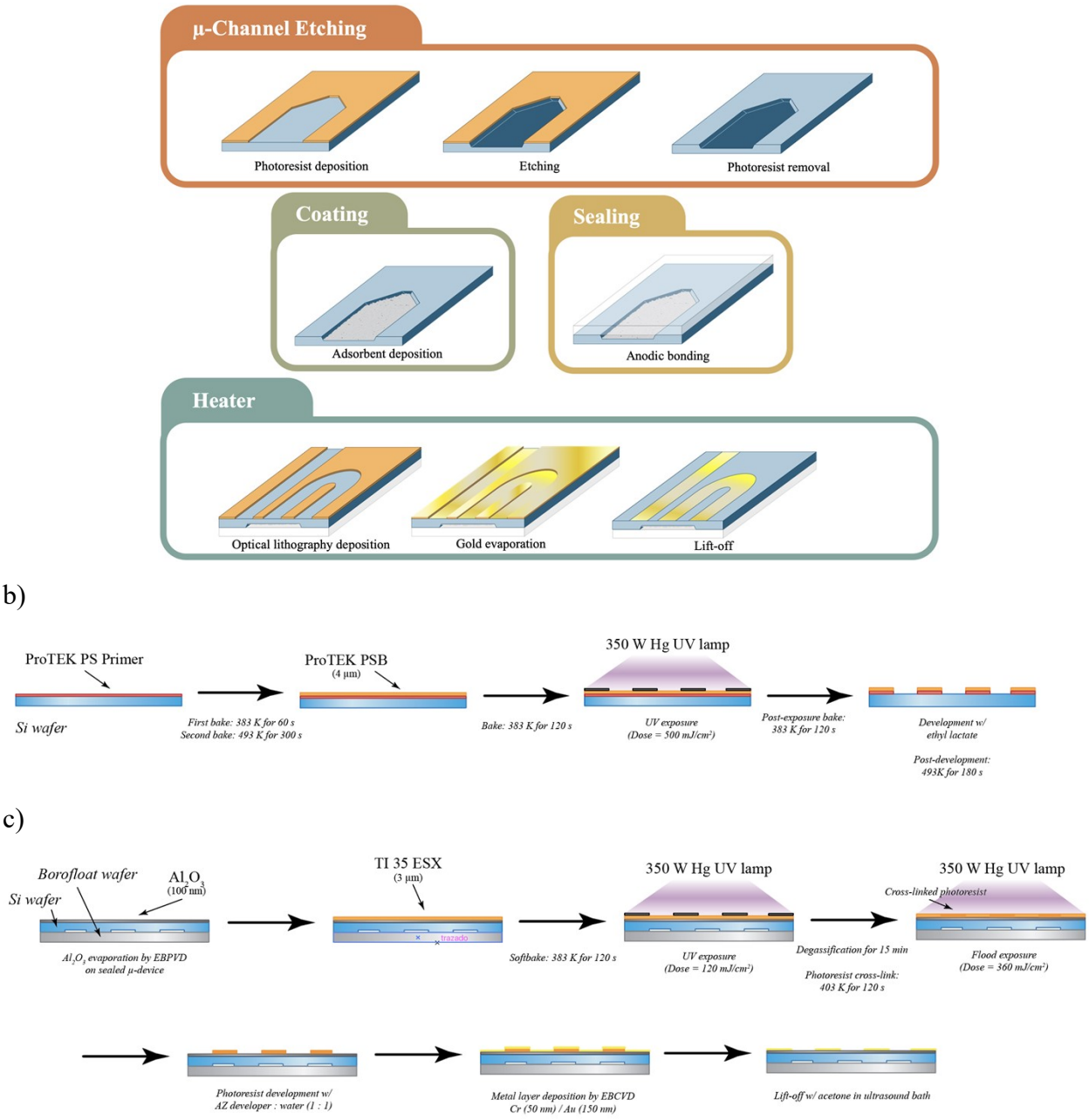

Figure S1.1 Fabrication of the microfluidic SERS chips: a) Schematic of the microdevice fabrication run; b) standard optical lithography process to define the microfluidic cavity; c) incorporation of Au heating coil and temperature sensing probe by standard lift-off process on the Si backside of the microfluidic chip.

Breakthrough Testing of the microfluidic SERS chip

Sorption dynamics of the functional microfluidic SERS chip was evaluated by analysis of the monitored breakthrough curve. A typical breakthrough curve, as depicted on Figure S11, follows the evolution in time or volume (of circulated gas) of the eluted analyte concentration downstream of the sorption unit. Mostly, the eluted concentration C_x is normalized by the feeding concentration C_0, so it ranges from 0 to 1.

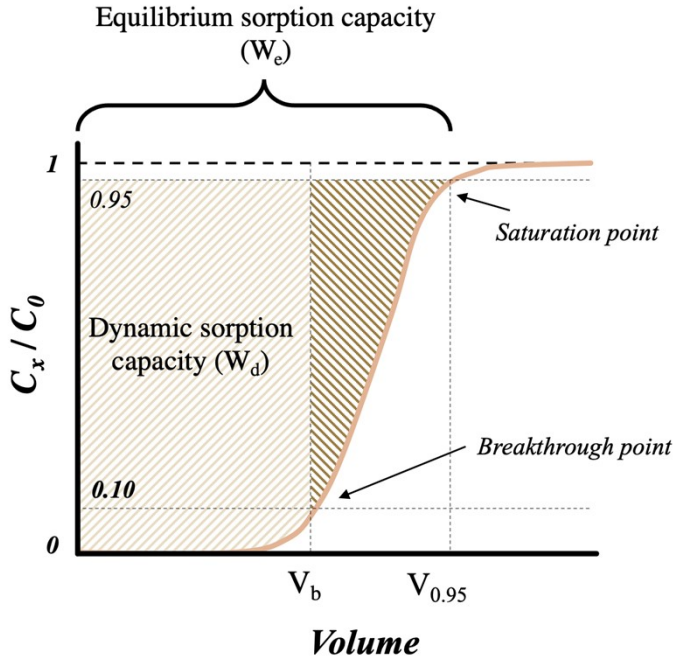

Figure S1.2. Typical breakthrough curve where the normalized concentration is plotted as a function of the volume that has been circulated inside the sorption unit.

For this work, breakthrough point is considered as the moment where $C_x/C_0 = 0.1$, which implies that the adsorbent is becoming saturated and begins to be unable to trap all the analyte molecules carried by the feeding gas. The moment at which breakthrough takes place is denoted as breakthrough time (t_b). Similarly, the volume that has been fed to the bed is defined as breakthrough volume ($V_b = t_b * Q_{feed}$, being Q_{feed}: feed volumetric flow).

The ratio of uptake sorbate (target analyte) mass up to breakthrough point (m_b) to the sorbent mass is defined as dynamic sorption capacity (W_d). Analogously, the point where the adsorbent is exhausted is denoted as saturation point; and in this work is assumed it takes places when $C_x/C_0 = 0.95$, this point determines the equilibrium sorption capacity when working in dynamic conditions (W_e). The maximum mass of sorbate can be calculated by integrated the area above of the breakthrough curve (up to $C_x/C_0 = 0.95$).

A conventional breakthrough test comprises the following steps (see Figure S1.3):

a) *Adsorbent pre-treatment*: before the adsorption experiment, the adsorbent is regenerated thermally by placing the microdevice on a hotplate at 200 ºC while inert N_2 sweeps the cavity and degas the sorptive layer. Ideally this step is performed until no undesirable specie was detected.

b) *Analyte baseline*: analyte was fed directly into the detector to obtain the baseline signal that is used for calibration. To avoid contamination on the adsorbent material, dry N_2 is circulated through the microdevice while this step takes place.

c) *Analyte adsorption:* analyte is fed to the microdevice until sorbent saturation, which is assessed by previous calibration ($C_{exit} = C_0$).

d) *Analyte desorption:* the analyte was desorbed under the same conditions as step 1.

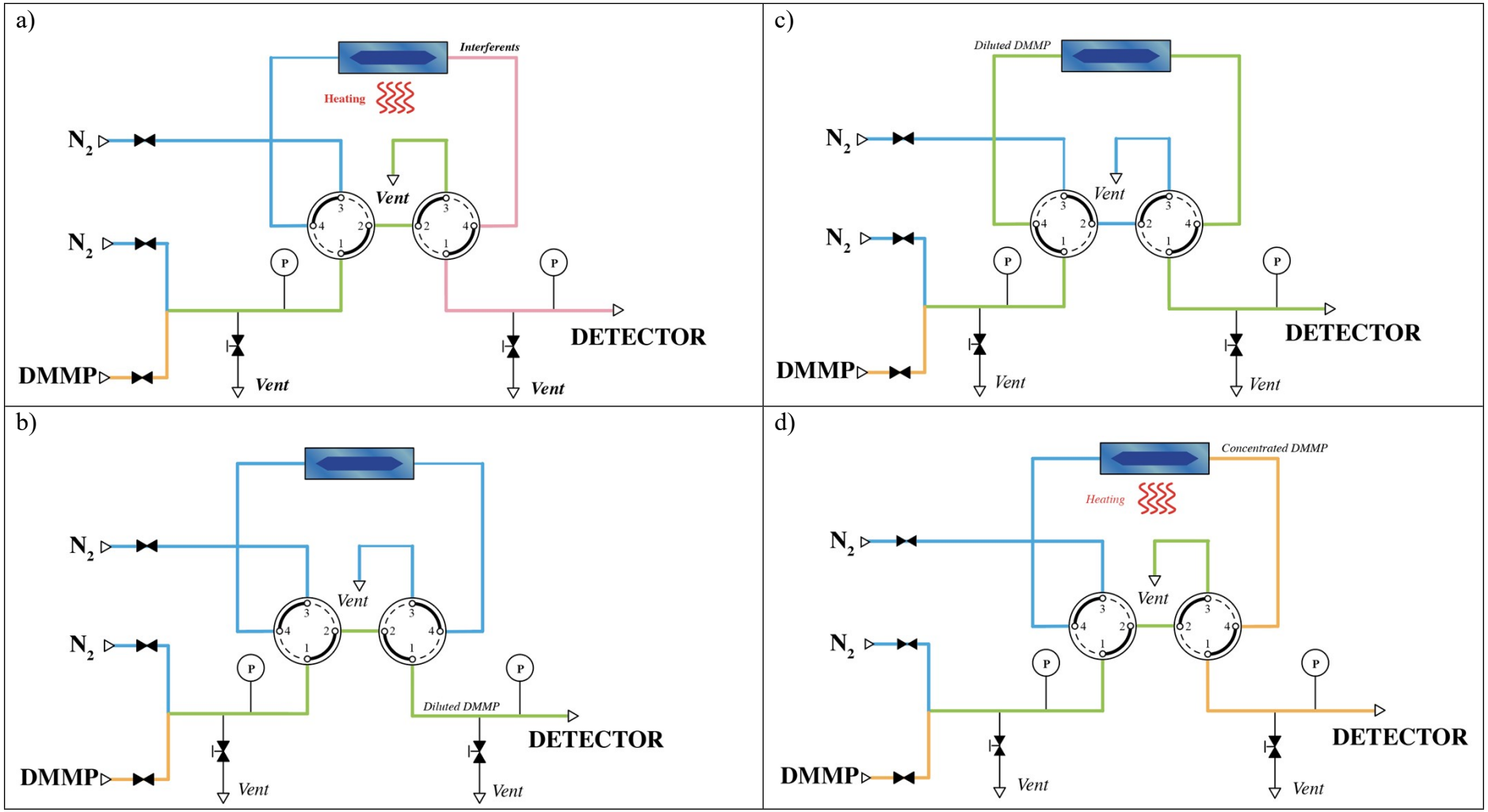

Figure S1.3. Scheme of flow arrangement in the experimental set-up for breakthrough testing: a) adsorbent pre-treatment, b) analyte baseline, c) analyte adsorption and d) analyte desorption.

Estimation of the thickness for the MCM48@Au coating of the microfluidic SERS chip

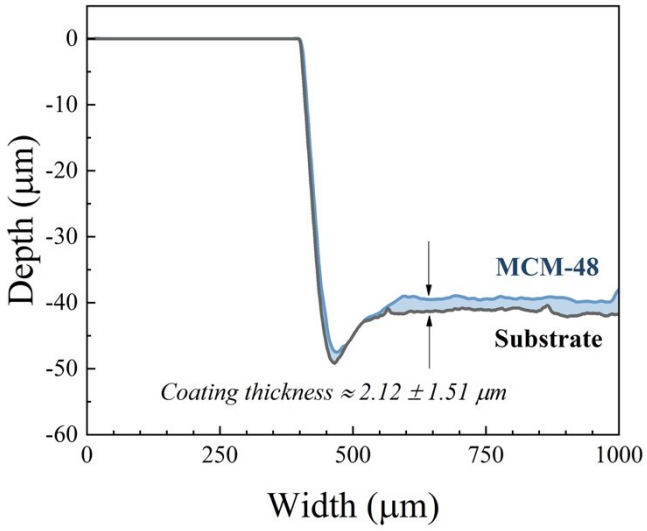

Figure S1.4. Profilometer analyses of MCM48@Au coating on the microfluidic SERS chip.

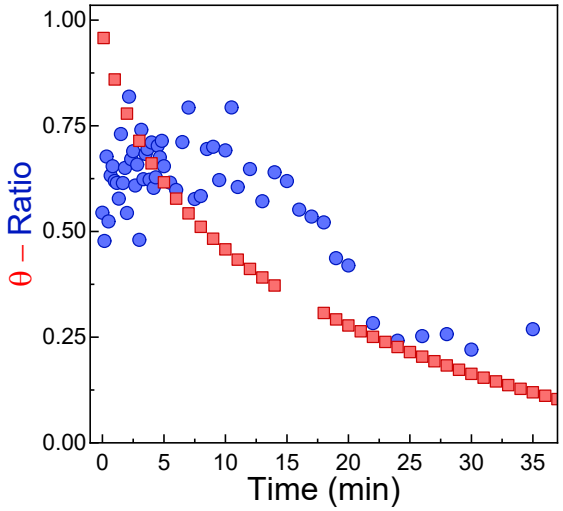

Figure S1.5. Monitoring of the DMMP desorption process from the microfluidic chip by the ratio-metric SERS signal acquired at 200ºC at the outlet of the chip (blue circles) and by GC-MS analysis of the outlet stream expressed as occupancy of sorption sites θ (red squares).

The occupancy of DMMP sorption sites, θ, is calculated from the macroscopic mass balance of DMMP in the chip, i.e., considering the gaseous molecules at the inlet, the molecules adsorbed on the plasmonic sorbent coating and the gaseous molecules in the outlet stream. By registering the DMMP concentration at the outlet, C_t during the desorption cycle at 200ºC with pure N_2, θ can be calculated as follows:

$$\theta = \frac{m_{tot,adsorbed} - m_{desorbed}}{m_{tot,\,adsorbed}} = 1 - \frac{Q}{W_e * m_{sorbent}} \int_{t_0}^{t} C_t dt \qquad \text{(Equation S1.1)}$$

where θ_t is the fraction of occupied DMMP sorption sites at a given time t, $m_{tot,adsorbed}$ is the total DMMP mass amount adsorbed by the active coating, $m_{desorbed}$ is the total amount of DMMP desorbed at a given time, W_e is the equilibrium capacity of the active coating, $m_{sorbent}$ is the mass of the active coating, C_t is the DMMP concentration at the outlet at a given time and Q is the N_2 flow rate.

Section 2. Synthesis and characterization of plasmonic silica-based sorbents

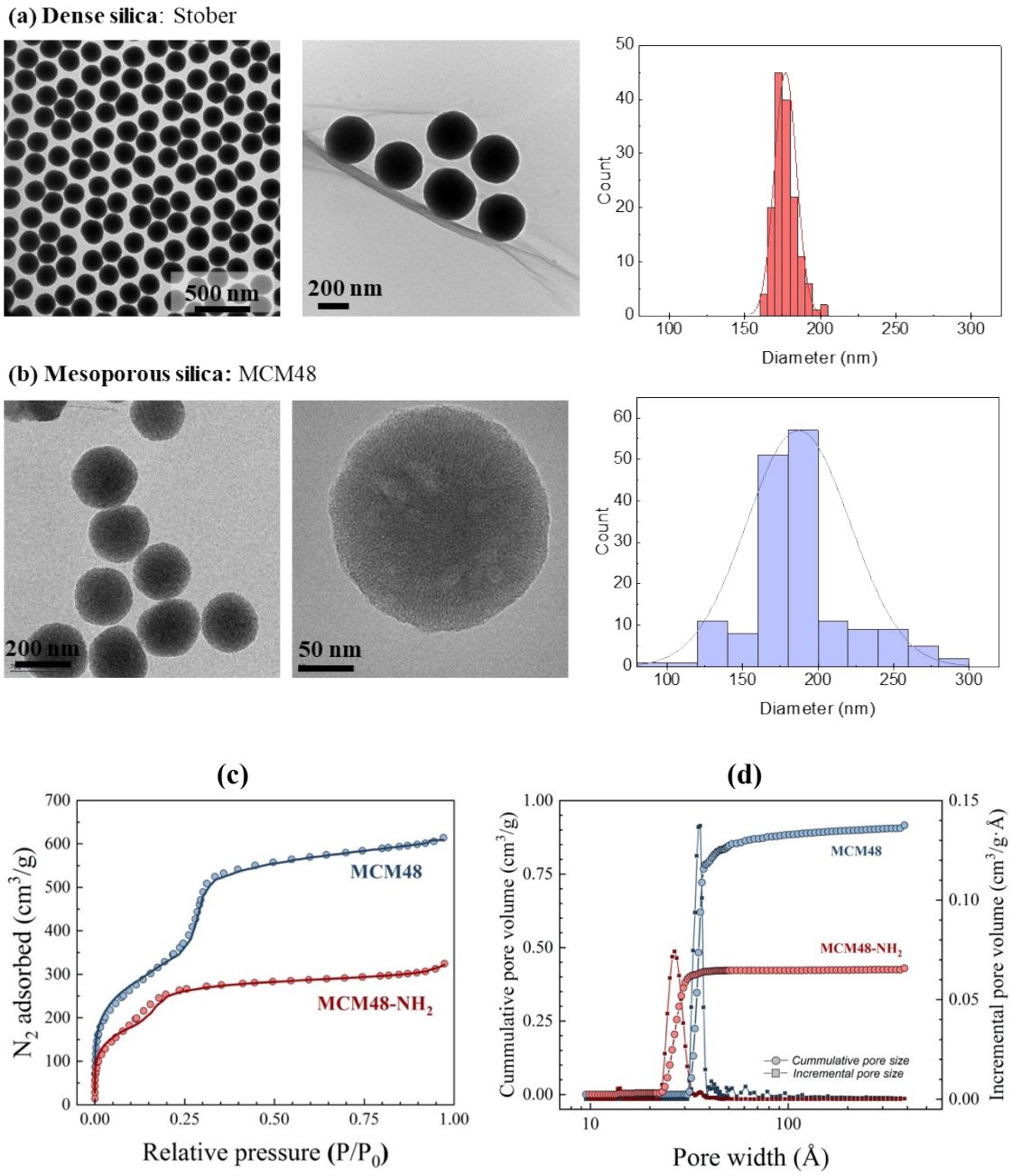

Figure S2.1. TEM images of **(a)** dense silica and **(b)** MCM48 nanoparticle with their corresponding diameter size distribution histograms (N>150). **(c)** Nitrogen physisorption analyses for MCM48 (blue) and amine-MCM48 (red) nanoparticles. **(d)** Pore volume distribution for MCM-48 (blue) and amine-MCM48 (red) nanoparticles (circles: cumulative pore volume, squares: incremental pore volume).

Table S2.1. Main textural properties of MCM48 type materials synthesized in this work.

Material	BET surface (m^2/g)	Pore volume (cm^3/g)	Pore size (nm)
MCM48	1237	0.96	3.5
MCM48-NH_2	1052	0.43	2.7

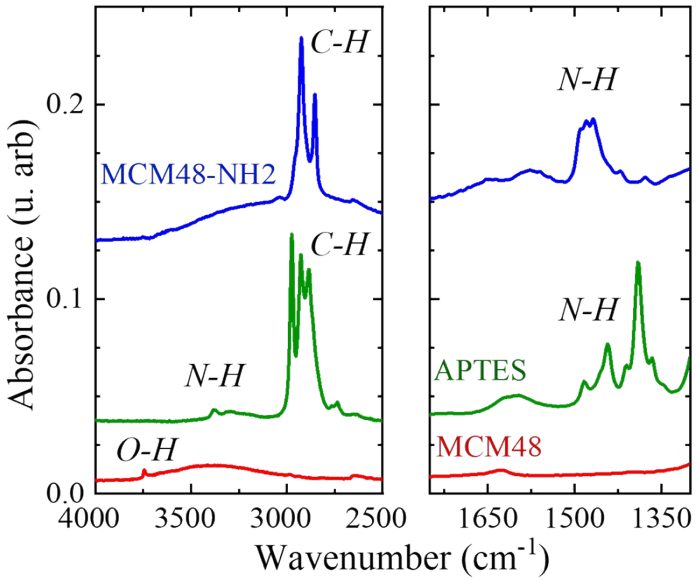

Figure S2.2. FTIR spectra of the MCM48 nanoparticles before and after amine-functionalization compared with APTES in liquid phase.

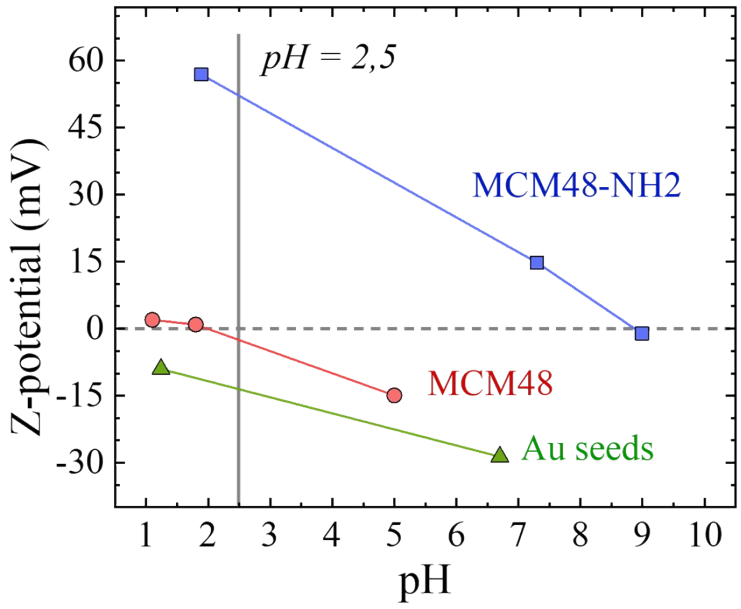

Figure S2.3. Z-potential of MCM48, MCM48-NH_2 and Au seeds aqueous solutions.

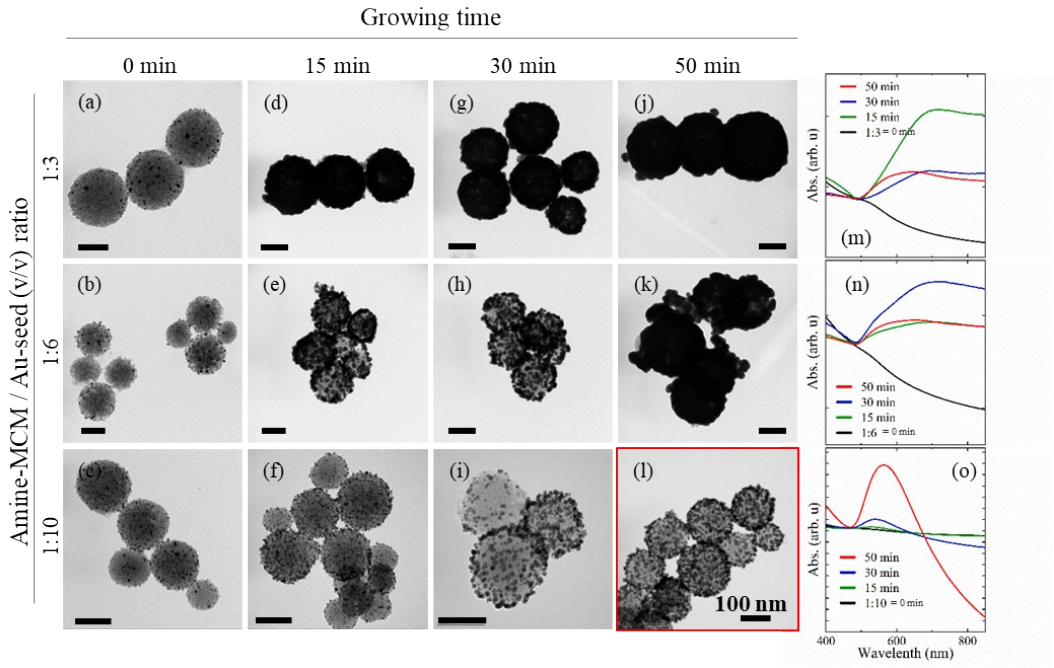

Figure S2.4. TEM images of the resulting nanoparticles along the synthesis process for the three amine-MCM48/Au seed ratios as a function of the Au seeds growing time (0, 15, 30 and 50 min) and normalized UV-Vis-NIR spectra of the aqueous solutions. Highlighted image in red (l) corresponds to the conditions selected as optimum for MCM48@Au synthesis. Scale bar represents 100 nm.

Figure S2.4 shows representative TEM images of the SERS probes for different ratios amine-MCM48/Au seed (1:3, 1:6 and 1:10) and growing times 15 to 50 minutes, together with the UV-Vis spectra. The same amount of Au precursor in the growing solution had different consequences depending on the seeds population of the silica surface, i.e. MCM48/Au seeds v/v ratio. In the case of MCM48/Au seeds_1:3 (Figure S2.4, first row), TEM images reveal the formation of a dense metallic shell even at the shortest reaction times, i.e.,15 min. On the other hand, growing times of 15 min and 30 min for MCM48/Au seeds_1:6 led to core-shell nanostructures with larger individual Au nanoparticles on the surface of MCM48 (Figure S2.4 (e)-(h)). These large Au nanoparticles continue growing up to completely seal the external shell at 50 min (Figure S2.4 (k)). The normalized extinction spectra for the samples of these two series (Figure S2.4 (m)-(n)) evidence the expected spectral shifting due to the plasmonic coupling between adjacent Au nanoparticles. In the case of the growth samples from MCM48/Au seeds_1:3 batch (Figure S2.4, third row), individual Au nanostructures are preserved along the growing period. As expected, the Au nanostructures on the surface of MCM48 spheres increase in size with reaction time (Figure S2.4 (f), (i), (l)). TEM observations agree with the increasing intensity of the resonant absorption feature at around 558 nm (Figure S2.4 (o)).

Figure S2.5 and Table S2.2 comparatively show the water and DMMP uptake of degassed samples before and after being exposed to 739 ppmV of DMMP in dry conditions at room temperature. DTA curve has being deconvoluted to better discriminate desorption events. The first weight-loss up to 50ºC is attributed to water desorption, whereas those shown at temperature above 50ºC are due to DMMP release. According to tabulated data, the higher DMMP uptake in static conditions is achieved by MCM48 (355 mg/g) which is in accordance to its textural properties (see Table S2.1)

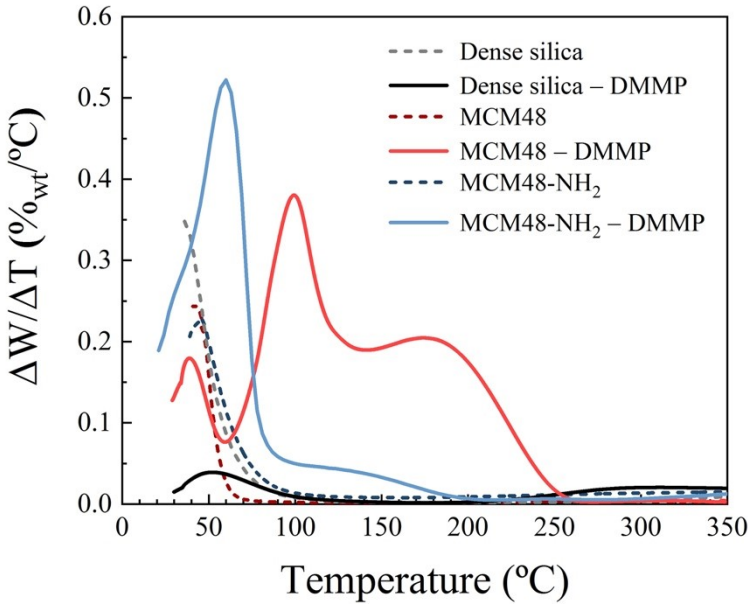

Figure S2.5. DMMP uptake values on silica-based samples estimated by TGA analyses.

Table S2.2. DTA Analyses of silica-based samples

Material	Control		After exposure to 739 ppmV DMMP					
	Δm mg/$g_{sorbent}$	T (ºC)	Δm mg/$g_{sorbent}$	T (ºC)	Δm mg/$g_{sorbent}$	T (ºC)	Δm mg/$g_{sorbent}$	T (ºC)
Dense SiO_2	66.8	36	21.5	52	-	-	-	-
MCM48	31.4	42	40.0	39	132.8	97	222.7	170
MCM48-NH_2	62.4	45	109.5	39	82.1	61	51.6	110

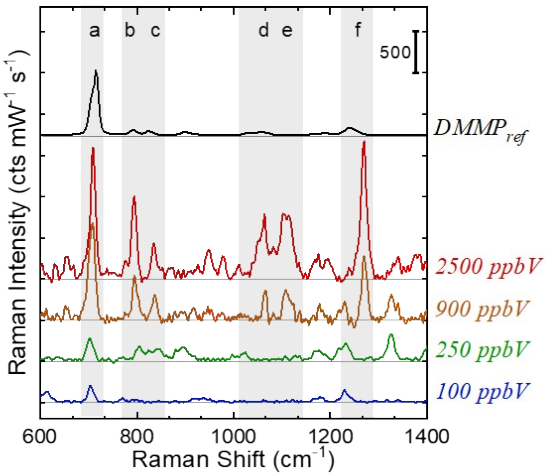

Figure S2.6. Average SERS spectra of different concentrations (100 – 2500 ppbV) of DMMP collected on MCM48@Au substrate. For better visualization, SERS spectra have been displaced in *y*-axis. Each concentration experiment was performed on a specific SERS substrate.

In Figure S2.6 when comparing the SERS spectra recorded for 100 and 250 ppbV with the rest, shifts in peak positions and variations in relative intensities are attributed to the gradual reordering of the adsorbed layers as the surface approaches saturation coverage[2].

Section 3. Optical and SERS Characterization of the silica@Au supported films

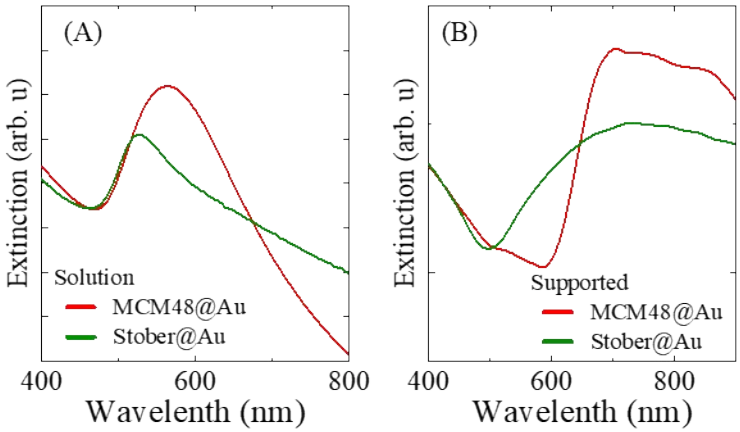

Figure S3.1. Comparison of UV-Vis-NIR spectra for (A) un-supported (aqueous solution) and (B) supported Stober@Au and MCM48@Au nanostructures on borofloat substrates.

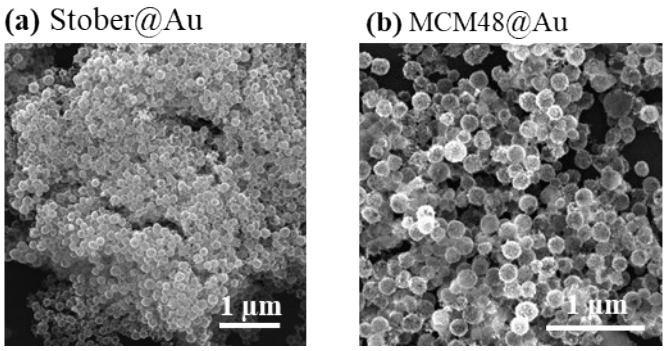

Figure S3.2. SEM analyses of supported (a) Stober@Au and (b) MCM48@Au nanostructures on Si/SiO substrates.

Determination of analytical enhancement factor (AEF).

Among the existed methods for the characterization of the SERS properties of a plasmonic substrate, we have selected the analytical enhancement factor (AEF)[3]. The AEF is defined by the following equation:

$$AEF = (I_{SERS} \times c_{Raman}) / (I_{Raman} \times c_{SERS}) \qquad \text{(Equation S3.1)}$$

where c_{Raman} and C_{SERS} are the Rhodamine 6G (R6G) concentration in the Raman measurements (1mM) and SERS conditions (1µM), respectively; I_{Raman} (cts mW^{-1} s^{-1}) is the intensity of R6G peak at 1510 cm^{-1} (C-C stretching mode) in the 1mM R6G solution; and, I_{SERS} (cts mW^{-1} s^{-1}) is the intensity of the same peak in the MCM48@Au SERS substrates with R6G 1 µM. Figure S3.3 illustratively shows the R6G SERS spectra recorded for both, MCM48@Au and Stober@Au films supported on Si/SiO_2 substrates.

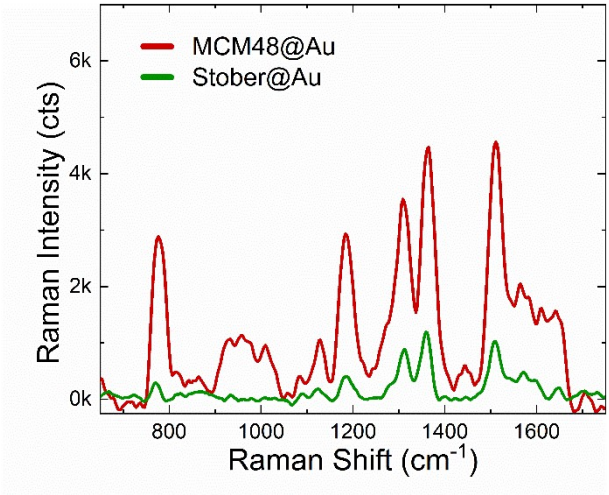

Figure S3.3. R6G SERS spectra (λ =7 85 nm) on MCM48@Au and Stober@Au nanostructures supported on Si/SiO_2 substrates.

A more detailed statistical analyses of the R6G experimental data set recorded on MCM48@Au and Stober@Au substrates has been performed using the "Student´s t-test" Accordingly, the confidence interval of 99% (α = 0.01) is calculated as follows:

$$m - \left(t_{n-1;\frac{\alpha}{2}}\right)\frac{s}{\sqrt{n}} < \mu < m + \left(t_{n-1;\frac{\alpha}{2}}\right)\frac{s}{\sqrt{n}}$$

or:

$$m \pm \left(t_{n-1;\frac{\alpha}{2}}\right)\frac{s}{\sqrt{n}}$$

where *m* is the sample mean; *s* is the sample standard deviation, *n* is the sample size, *n-1* is the degrees of freedom and μ is the real population mean. Table S3.1. compiles our experimental results, the calculated $\left(t_{n-1;\frac{\alpha}{2}}\right)$ values using Excel (function *¨dist.t.inv¨*), and the related parameters thereof.

Table S3.1. "Student´s t-test" analyses of the R6G SERS peak (at 1510 cm^{-1}) for 99% confidence interval recorded on MCM48@Au and Stober@Au substrates.

	Data Set 1	Data Set 2
Name ID	MCM48@Au	Stober@Au
m	4556	1029
s	780	240
n	25	20
n-1	24	19
α	0.01	0.05
t	$(t_{24;0.005}) = 2.797$	$(t_{19;0.005}) = 2.861$
$\left(t_{n-1;\frac{\alpha}{2}}\right)\frac{s}{\sqrt{n}}$	436	154
$m \pm \left(t_{n-1;\frac{\alpha}{2}}\right)\frac{s}{\sqrt{n}}$	4556 ± 436	1029 ± 154

Accordingly, it can be inferred that there is a 99% probability to find the mean of R6G SERS intensity at 1510 cm^{-1} within (4126, 4992) and (875-1183) intervals for both "MCM48@Au" and "Stober@Au" populations, respectively. Thus, we can conclude that there is a significant difference between the SERS performance of these two substrates.

Table S3.2. Experimental vibrational frequencies of pure DMMP (liquid), DMMP (gas phase at ppmV level) recorded on MCM48@Au and tentative assignments.

Band ID.	**Raman Shift (cm^{-1})**		**Vibrational assigments**[4]
	Pure DMMP	**DMMP on MCM48@Au**	
a	**718**	**710**	**P-CH_3 *stretching***
b	794	793	PO_2 *bending*
c	825	835	PO_2 *bending*
d	1039	1064	C-O *stretching*
e	1062	1107	C-O *stretching*

f	1240	1270	P=O *stretching* CH_3 *bending*

References

1 F. Almazán, I. Pellejero, A. Morales, M. A. Urbiztondo, J. Sesé, M. P. Pina and J. Santamaría, *Journal of Micromechanics and Microengineering*, 2016, **26**, 084010.

2 K. B. Biggs, J. P. Camden, J. N. Anker and R. P. V. Duyne, *Journal of Physical Chemistry A*, 2009, **113**, 4581–4586.

3 E. C. le Ru, E. Blackie, M. Meyer and P. G. Etchegoint, *Journal of Physical Chemistry C*, 2007, **111**, 13794–13803.

4 J. C. S. Costa, R. A. Ando, A. C. Sant'Ana and P. Corio, *Physical Chemistry Chemical Physics*, 2012, **14**, 15645–15651.